

Generation of Physically Consistent Fission Yields Using a Bayesian Approach

YuGwon Jo^{a*}, Jaewoon Yoo^a, and Jae-Yong Lim^a

^aKorea Atomic Energy Research Institute, 989-111 Daedeok-daero, Yuseong-gu, Daejeon, Korea, 34057

*Corresponding author: yugwonjo@kaeri.re.kr

*Keywords : Fission Yield, Bayesian, Generalized Least Squares, Negative Fixup

1. Introduction

Fission product yields are important nuclear data for the reactor design and operation, as well as spent fuel management [1]. The fission yield data is provided in MF=8 of the evaluated nuclear data file (ENDF), where independent yields are given in MT=454 and cumulative yields in MT=459, along with their uncorrelated (individual) uncertainties [2]. However, the fission yields of the ENDF often lack the physical consistence, such as mass and charge conservation, asymmetry, and binarity, as they are compiled from the individually conducted experiments.

There have been several studies [3-6] to resolve the inconsistent fission yields by using a Bayesian generalized least squares method (B-GLSM) and obtain covariance of fission yields. However, the application of the B-GLSM often leads to the occurrence of negative fission yields.

This paper investigates the several negative fission yield fixup methods for the B-GLSM. The performances of the negative fixup methods were compared in terms of the cost function derived from the physical constraints. Then, the impact of the updated fission yields was investigated through the depletion of a typical 17x17 light water reactor (LWR) fuel assembly.

2. Methodology

2.1. Bayesian Generalized Least Squares Method (B-GLSM)

Four physical constraints on independent fission yields, summarized in Table I, are considered in this study. In Table I, N_{FP} is the total number of fission products (FPs), the subscript i is the index of FP, the subscript CN indicates the compound nucleus, Y is the fission yield, Z is the atomic number, A is the mass number, $\nu_p(E)$ is the number of prompt fission neutrons per fission at incident neutron energy E , $\sigma[\nu_p(E)]$ is the uncertainty of the $\nu_p(E)$, and HCP indicates the heavy charged particles with $Z > 10$. Note that $\nu_p(E)$ and $\sigma[\nu_p(E)]$ are provided in the (MF=1, MT=456) and (MF=31, MT=456), respectively. The terms on the right side of equations are treated as observations with uncertainties.

Based on the constraints, the design matrix equation can be formulated as:

$$\mathbf{X}\boldsymbol{\beta}_{prior} + \mathbf{e} = \mathbf{y}_m, \quad (1)$$

Table I. Physical constraints of fission yields

Physical Meaning	Equation	Observations and Uncertainties
Charge Conservation	$\sum_{i=1}^{N_{FP}} Z_i Y_i = Z_{CN}$	$Z_{CN} \pm 0.00\%$
Mass Conservation	$\sum_{i=1}^{N_{FP}} A_i Y_i = A_{CN} - \nu_p(E)$	$A_{CN} - \nu_p(E) \pm \sigma[\nu_p(E)]$
Asymmetry	$\sum_{A_i > \frac{A_{CN} - \nu_p(E)}{2}} Y_i = 1$	$1 \pm 0.00\%$
Binarity	$\sum_{i \in HCP} Y_i = 2$	$2 \pm 0.00\%$

where \mathbf{X} is the design matrix, $\boldsymbol{\beta}_{prior}$ is the prior independent fission yields provided in the ENDF, \mathbf{y}_m is the observation, which are defined, respectively, as:

$$\mathbf{X} = \begin{bmatrix} Z_1 & Z_2 & \cdots & Z_{N_{FP}} \\ A_1 & A_2 & \cdots & A_{N_{FP}} \\ a_1 & a_2 & \cdots & a_{N_{FP}} \\ b_1 & b_2 & \cdots & b_{N_{FP}} \end{bmatrix}, \quad (2)$$

$$\boldsymbol{\beta}_{prior} = [Y_1 \quad Y_2 \quad \cdots \quad Y_{N_{FP}}]^T, \quad (3)$$

$$\mathbf{y}_m = [Z_{CN} \quad A_{CN} - \nu_p(E) \quad 1 \quad 2]^T, \quad (4)$$

and \mathbf{e} is the error of the regression model.

Then, the B-GLSM is applied to minimize the cost function defined as:

$$C(\boldsymbol{\beta}) = (\boldsymbol{\beta} - \boldsymbol{\beta}_{prior})^T \mathbf{V}_{prior}^{-1} (\boldsymbol{\beta} - \boldsymbol{\beta}_{prior}) + (\mathbf{y}_m - \mathbf{X}\boldsymbol{\beta})^T \mathbf{V}_m^{-1} (\mathbf{y}_m - \mathbf{X}\boldsymbol{\beta}), \quad (5)$$

where

$$\mathbf{V}_{prior} = \text{diag}([\sigma^2(Y_1) \quad \sigma^2(Y_2) \quad \cdots \quad \sigma^2(Y_{N_{FP}})]), \quad (6)$$

$$\mathbf{V}_m = \text{diag}([0 \quad \sigma^2(v_p(E)) \quad 0 \quad 0]). \quad (7)$$

The posterior fission yields that minimize the cost function are determined as Eq. (8), and their covariance matrix is given by Eq. (9), as follows:

$$\boldsymbol{\beta}_{post} = \boldsymbol{\beta}_{prior} + \mathbf{V}_{prior} \mathbf{X}^T (\mathbf{V}_m + \mathbf{X} \mathbf{V}_{prior} \mathbf{X}^T)^{-1} (\mathbf{y}_m - \mathbf{X} \boldsymbol{\beta}_{prior}), \quad (8)$$

$$\mathbf{V}_{post} = \mathbf{V}_{prior} - \mathbf{V}_{prior} \mathbf{X}^T (\mathbf{V}_m + \mathbf{X} \mathbf{V}_{prior} \mathbf{X}^T)^{-1} \mathbf{X} \mathbf{V}_{prior}. \quad (9)$$

2.2. Negative Fixup Methods

Figure 1 shows the occurrence of the negative posterior fission yields obtained by the B-GLSM. To prevent the negative fission yields, several negative fixup methods described in Table II were implemented.

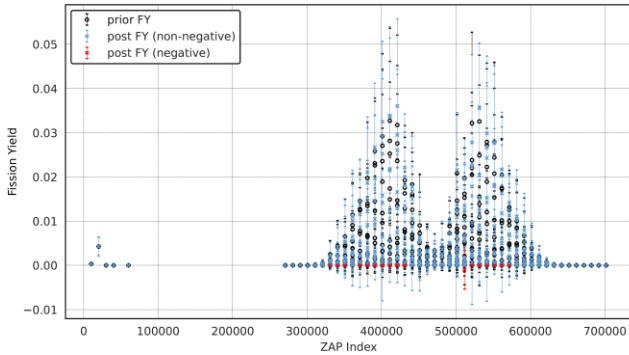


Figure 1. Prior and posterior fission yields of Pu-242 induced by neutrons with $E_n=14$ MeV by the B-GLSM; The error bars indicate 1-sigma uncertainties and red markers highlight negative posterior fission yields.

Table II. Negative fixup methods for B-GLSM

Methods	Description
Zero Fixup	Step 1. Apply B-GLSM to evaluate $\boldsymbol{\beta}_{post}$. Step 2. Fix negative yields to zero.
Prior Fixup	Step 1. Apply B-GLSM to evaluate $\boldsymbol{\beta}_{post}$. Step 2. Fix negative yields to prior yields.
Iterative Zero Fixup	Step 1. Apply B-GLSM to evaluate $\boldsymbol{\beta}_{post}$. Step 2. If negative yields occur, fix them to zero, otherwise terminate the process. Step 3. Apply B-GLSM for unfixed elements to evaluate $\boldsymbol{\beta}_{post}$ and go to Step 2.
Iterative Prior Fixup	Step 1. Apply B-GLSM to evaluate $\boldsymbol{\beta}_{post}$. Step 2. If negative fission yields occur, set them to prior yields, otherwise terminate. Step 3. Apply B-GLSM for unfixed elements to evaluate $\boldsymbol{\beta}_{post}$ and go to Step 2.
L-BFGS-B Algorithm	Apply the constrained nonlinear optimization algorithm (L-BFGS-B [7]) from <i>scipy.optimize</i> package [8].

3. Results

3.1. Update of Fission Yields

The prior fission yield is taken from the fission yield library of the McCARD, the Monte Carlo (MC) reactor analysis code [9]. The McCARD fission yield library is compiled as follows. First, 880 fission product isotopes are selected based on the ORIGEN2 yield library [10]. Then, independent fission yields were taken from these of 31 fissionable nuclides provided in ENDF-349 [11]. For ternary fission products, H-3 and He-4 are sourced from Ref. [11], while the remaining ternary fission products Li-6, Li-7, Be-9, Be-10, and C-14 are from the ORIGEN2 yield library.

The standard deviations of the prior fission yields are taken from Ref. [11]. Since the ORIGEN yield library does not provide uncertainty, the uncertainty of the ternary fission products sourced from the ORIGEN2 is set to 64%, which corresponds to the maximum relative standard deviation in Ref. [11].

The performance of the B-GLSM with negative fixup methods were compared in Table III. Among the tested methods, the iterative zero fixup method yields the minimum cost.

Table III. Negative fixup methods for B-GLSM

Methods	Total Cost (31 nuclides)
Prior Value	661,000
B-GLSM (No Fixup)	4,233
Zero Fixup	35,910,660
Prior Fixup	485,385,053
Iterative Zero Fixup	4,402
Iterative Prior Fixup	607,995
L-BFGS-B Algorithm	10,964

Four residuals were calculated to check the improvement by the B-GLSM, defined as follows:

$$\text{Residual}_1 = \sum_{i=1}^{N_{FP}} Z_i Y_i - Z_{CN}, \quad (10)$$

$$\text{Residual}_2 = \sum_{i=1}^{N_{FP}} A_i Y_i - (A_{CN} - v_p(E)), \quad (11)$$

$$\text{Residual}_3 = \sum_{A_i > \frac{A_{CN} - v_p(E)}{2}} Y_i - 1, \quad (12)$$

$$\text{Residual}_4 = \sum_{Z_i \in HCP} Y_i - 2. \quad (13)$$

When the residuals are close to 0.0, the fission yields satisfy the physical constraint. The four residuals of 31 fissionable nuclides are displayed in Figure 2. Except for the mass conservation constraint, which was relaxed by $\sigma[v_p(E)]$, the other constraints were effectively satisfied.

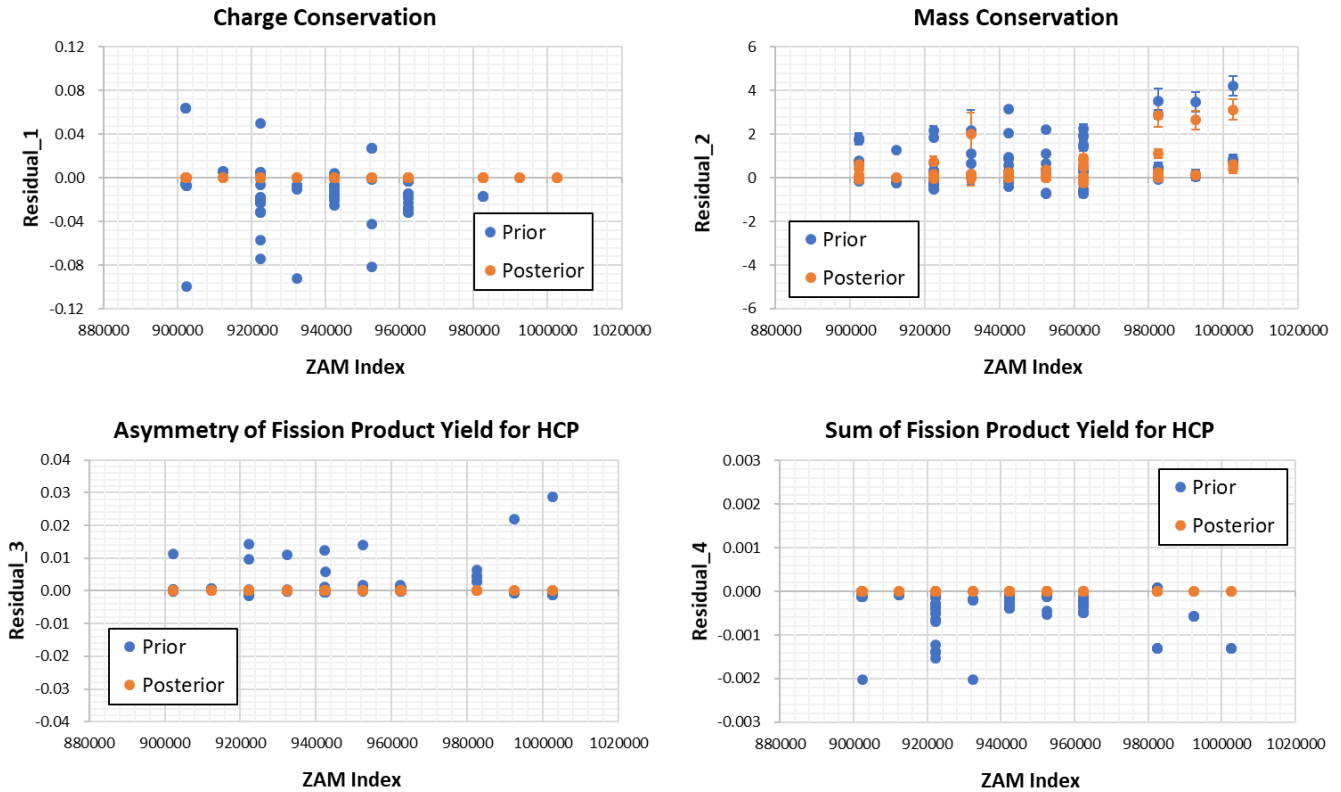


Figure 2. Improved fission yields by the B-GLSM with iterative zero fixup; ZAM index is defined as $Z \times 10^4 + A \times 10 + M$ with Z, A, and M corresponding to the atomic number, mass number, and metastable state of fissioning nuclide, the error bars indicate 2-sigma.

The prior and posterior fission yields of Pu-242 induced by neutrons with $E_n=14$ MeV by the B-GLSM with iterative zero fixup are shown in Figure 3 and their covariance matrices are also provided in Figure 4. Compared to the posterior fission yields shown in Figure 1, the negative fission yields are fixed up in Figure 3. In Figure 4, the prior covariance matrix consists of only the diagonal elements, whereas the posterior covariance matrix includes off-diagonal elements that introduce negative correlations, thereby reduces the uncertainties.

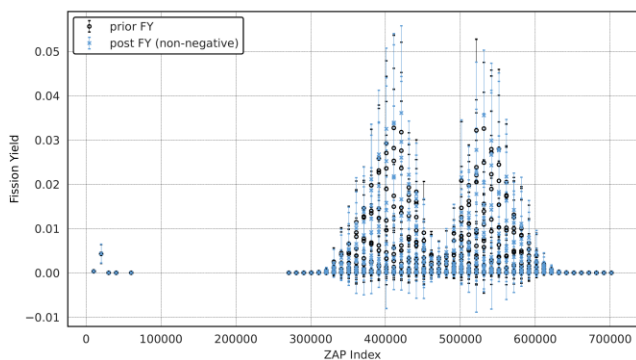


Figure 3. Prior and posterior fission yields of Pu-242 induced by neutrons with $E_n=14$ MeV by the B-GLSM with

iterative zero fixup; The error bars indicate 1-sigma uncertainties.

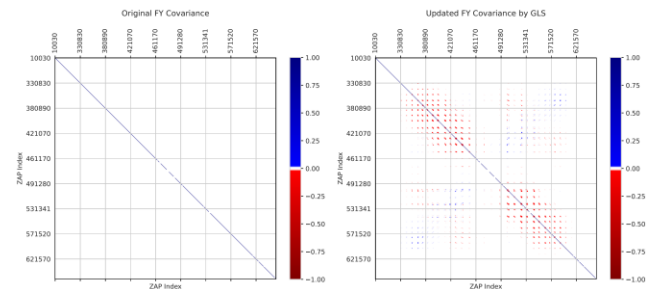


Figure 4. Prior (left) and posterior (right) covariance matrices of fission yields of Pu-242 induced by neutrons with $E_n=14$ MeV; ZAP index is defined as $Z \times 10^4 + A \times 10 + M$ with Z, A, and M corresponding to the atomic number, mass number, and metastable state of fission product.

Table IV presents the prior and posterior fission yields of xenon chain isotopes from U-235 at incident neutron energy of 0.0253 eV. The total xenon yield increases around 1%, which can be crucial for the criticality calculation especially for the LWR spectrum.

Table IV. Prior and posterior fission yields of xenon chain isotopes from U-235 induced by neutrons with $E_n=0.0253$ eV

Fission Products	Prior (A)	Posterior (B)	Rel. Diff. (B/A-1) [%]
Te-135	3.216	3.273	1.8
I-135	2.928	2.929	0.0
Xe-135m	0.178	0.178	-0.1
Xe-135	0.079	0.078	0.0
Total	6.401	6.458	0.9

3.2. Depletion Calculation Result

For a typical 17x17 LWR fuel assembly with U-235 enrichment of 4.0 wt%, the depletion calculation was performed by the McCARD with prior and posterior fission yield libraries. Table V and Table VI show Xe-135 number density and the keff with prior and posterior fission yield libraries, respectively. The xenon number density increases 0.4 % and keff decreases around 10 pcm with posterior fission yield library.

Table V. Comparisons of Xe-135 number density with prior and posterior fission yield libraries

Day	Prior (A)	Posterior (B)	Rel. Diff. (B/A-1) [%]
0	0.000E+00	0.000E+00	-
3	9.848E-06	9.889E-06	0.42
30	6.715E-06	6.743E-06	0.41
60	6.724E-06	6.751E-06	0.40
90	6.736E-06	6.762E-06	0.40
120	6.746E-06	6.772E-06	0.39
150	6.755E-06	6.780E-06	0.38
180	6.763E-06	6.788E-06	0.37
210	6.770E-06	6.795E-06	0.37
240	6.777E-06	6.802E-06	0.36

Table VI. Comparisons of keff with prior and posterior fission yield libraries

Day	Prior (A)	Posterior (B)	Δ keff (B-A) [pcm]
0	1.38024 ± 0.00002	1.38024 ± 0.00002	0.0 ± 2.8
3	1.34792 ± 0.00002	1.34780 ± 0.00002	-12.0 ± 2.8
30	1.35003 ± 0.00002	1.34993 ± 0.00002	-10.0 ± 2.8
60	1.34470 ± 0.00002	1.34461 ± 0.00002	-9.0 ± 2.8
90	1.34088 ± 0.00002	1.34077 ± 0.00002	-11.0 ± 2.8
120	1.33767 ± 0.00002	1.33753 ± 0.00002	-14.0 ± 2.8
150	1.33463 ± 0.00002	1.33453 ± 0.00002	-10.0 ± 2.8
180	1.33171 ± 0.00002	1.33158 ± 0.00002	-13.0 ± 2.8
210	1.32875 ± 0.00002	1.32868 ± 0.00002	-7.0 ± 2.8
240	1.32584 ± 0.00002	1.32568 ± 0.00002	-16.0 ± 2.8

4. Summary and Conclusions

The application of the B-GLSM to impose the physical constraints on the fission yields leads to the occurrence of

the negative fission yields. Several negative fixup methods were tested and the iterative zero fixup method proposed in this study showed the best performance in terms of cost function. The impact of the updated fission yield was also investigated through the depletion of the single fuel assembly. The results showed that the around 10 pcm decrements compared to the original fission yield library.

Acknowledgement

This work was supported by the National Research Foundation of Korea (NRF) grant funded by the Korea government (MSIT). (No. RS-2022-00155157).

REFERENCES

- [1] IAEA, Compilation and evaluation of fission yield nuclear data, IAEA-TECDOC-1168, IAEA, December 2000.
- [2] CSEWG, ENDF-6 Formats Manual, National Nuclear Data Center, Brookhaven National Laboratory, July 2000.
- [3] M.T. Pigni et al., "Investigation of Inconsistent ENDF/B-VII.1 Independent and Cumulative Fission Product Yields with Proposed Revisions," Nuclear Data Sheets, vol. 123, pp. 231-236, 2015.
- [4] N. Terranova et al., "A Covariance Generation Methodology for Fission Product Yields," EPJ Web of Conferences, vol. 111, 09003, 2016.
- [5] L. Fiorito et al., "Generation of fission yield covariances to correct discrepancies in the nuclear data libraries," Annals of Nuclear Energy, vol. 88, pp. 12-23, 2016.
- [6] O. Leray et al., "Nuclear data uncertainty propagation on spent fuel nuclide compositions," Annals of Nuclear Energy, vol. 94, pp. 603-611, 2016.
- [7] C. Zhu, et al., "Algorithm 778: L-BFGS-B: Fortran Subroutines for Largs-Scale Bound-Constrained Optimization," ACM Transactions on Mathematical Software, Vol. 23(4), pp. 550-560, 1997.
- [8] P. Virtanen, et al., "Scipy 1.0: fundamental algorithms for scientific computing in Python," Nature Methods, vol. 17, pp. 261-272, 2020.
- [9] H. Shim, et. al., "McCARD: Monte Carlo Code for Advanced Reactor Design and Analysis," *Nuclear Engineering and Technology*, vol. 44, pp. 161-176, 2012.
- [10] A. G. Croff. "A User's Manual for ORIGEN2 Computer Code," ORNL/TM-7175, Oak Ridge National Laboratory (1980)
- [11] T. R. England and B. F. Rider, "Evaluation and Compilation of Fission Product Yields 1993," ENDF-349, LA-UR-94-3106, Los Alamos National Laboratory, USA, October, 1994.